ISME

www.nature.com/ismej

ARTICLE

Wet-dry cycles protect surface-colonizing bacteria from major antibiotic classes

Yana Beizman-Magen[1,2], Maor Grinberg[1,2], Tomer Orevi[1] and Nadav Kashtan[1]✉

Diverse antibiotic compounds are abundant in microbial habitats undergoing recurrent wet-dry cycles, such as soil, root and leaf surfaces, and the built environment. These antibiotics play a central role in microbial warfare and competition, thus affecting population dynamics and the composition of natural microbial communities. Yet, the impact of wet-dry cycles on bacterial response to antibiotics has been scarcely explored. Using the bacterium *E. coli* as a model organism, we show through a combination of experiments and computational modeling, that wet-dry cycles protect bacteria from beta-lactams. This is due to the combined effect of several mechanisms including tolerance induced by high salt concentrations and slow cell-growth, which are inherently associated with microscopic surface wetness—a hydration state typical to 'dry' periods. Moreover, we find evidence for a cross-protection effect, where lethal doses of antibiotic considerably increase bacterial survival during the dry periods. This work focuses on beta-lactams, yet similar protection was observed for additional major antibiotic classes. Our findings shed new light on how we understand bacterial response to antibiotics, with broad implications for population dynamics, interspecies interactions, and the evolution of antibiotic resistance in vast terrestrial microbial habitats.

The ISME Journal (2022) 16:91–100; https://doi.org/10.1038/s41396-021-01051-4

INTRODUCTION

A large portion of bacterial life occurs on surfaces that are not constantly saturated with water and experience recurrent wet-dry cycles characterized by 'dry' periods of very low water potential [1–3]. Bacteria on these surfaces are exposed to diverse natural and synthetic antibiotic compounds. Antibiotics are abundant in soil, root, and leaf surfaces, due to their natural production by microorganisms and plants [4–10], and their release into water and soil by human activity and agricultural practices [11–13]. These antibiotics play a major role in interspecies competition and microbial warfare [8–10], and therefore affect population dynamics and the structure of microbial communities [14–17]. Yet, little is known about how wet-dry cycles affect bacterial response to antibiotics.

Bacteria respond to the presence of antibiotics in various ways. Resistance to antibiotics is the (usually inherited) ability of bacteria to grow under high antibiotic concentrations, i.e., above the minimum inhibitory concentration (MIC) [18, 19]. Tolerance is the ability of a microorganism to survive a transient exposure to an antibiotic at concentrations that would otherwise be lethal (i.e., above the MIC) [18, 20, 21]. Tolerance may result from the physiological states of individual cells or from the collective properties of populations [18, 21–24], and can be thought of as transient protection that emerges under environmental conditions that impose low metabolic activity and reduced growth. Two common types of tolerance were identified: 'tolerance by slow growth', which stems from conditions that reduce cell-growth rates; and 'tolerance by lag', which occurs in growth-arrested cells during the lag phase [18].

To begin to understand the bacterial response to antibiotics under wet-dry cycles, we chose to focus on beta-lactams—one of the most well-studied and commonly used antibiotics [25–30]. Beta-lactams target penicillin-binding proteins in bacterial cell membranes that are responsible for crosslinking peptidoglycan layers, resulting in accumulated damage to cell membrane that eventually leads to cell lysis. In addition to their clinical importance, diverse groups of beta-lactams are abundant in terrestrial microbial habitats, where they are produced by many bacteria and fungi [7, 27].

During 'dry' periods, while many surfaces undergoing wet-dry cycles may appear dry to the naked eye, they are typically covered by thin liquid films and micrometer-sized droplets, termed microscopic surface wetness [2, 31, 32] (MSW; Fig. 1). Key to the formation and retention of microscopic wetness is the presence of deliquescent substances—mostly highly hygroscopic salts—that absorb moisture from the air until they dissolve-in and form a liquid solution [32–34]. Thus, residual deposits of deliquescent compounds that cover a surface are retained as, or become, MSW when the relative humidity (RH) exceeds their efflorescence, or deliquescence, points [33, 34]. As deliquescent substances are ubiquitous, MSW occurs in many microbial habitats that undergo wet-dry cycles, including plant root and leaf surfaces [2, 35, 36], soil and rock surfaces [37, 38], the built environment [39, 40], and probably even on human and animal skin [41].

[1]Institute of Environmental Sciences, Department of Plant Pathology and Microbiology, Robert H. Smith Faculty of Agriculture, Food, and Environment, Hebrew University, Rehovot 76100, Israel. [2]These authors contributed equally: Yana Beizman-Magen, Maor Grinberg. ✉email: nadav.kashtan@mail.huji.ac.il

Received: 21 January 2021 Revised: 24 June 2021 Accepted: 25 June 2021
Published online: 12 July 2021

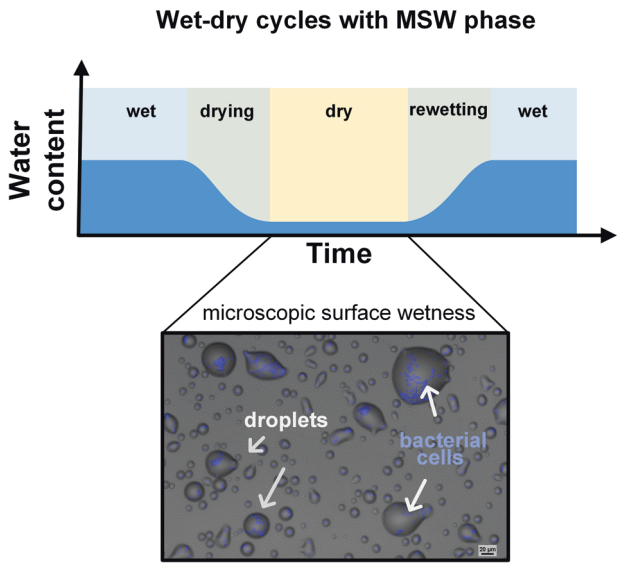

Fig. 1 Wet-dry cycles are prevalent in the largest terrestrial microbial habitats. A schematic depiction of a wet-dry cycle. Gradual water evaporation during the drying phase results, under many environmental circumstances, in the formation of microscopic surface wetness (MSW). Inset shows examples of fluorescently labeled bacteria in microscopic surface wetness that formed from drying of M9 medium. Bacterial cells reside within stable micrometer-sized droplets. Solutions in droplets are highly concentrated (high salinity); cells are stressed, and growth rates are low.

MSW can protect bacteria from complete desiccation [31]. For example, MSW resulting from the deliquescence of hygroscopic aerosols—which are ubiquitous on leaves [42, 43]—may explain how bacteria survive daytime dryness on plant leaves [31, 44]. MSW's physicochemical properties, such as extremely high salinities, altered pH, increase in reactive oxygen species (ROS), and segregation into tiny droplets [45–47], necessarily impose severe stresses on cells, and thus significantly impact the physiology of bacterial cells therein [48–50]. Cells that are exposed to drying and MSW were shown to activate stress responses [51] and exhibit very low, or even close to zero, growth rates [31].

Two key properties of MSW as a microbial environment—slow bacterial growth rates and high salt concentrations—have been shown to increase tolerance and reduce susceptibility to antibiotics [52–58]. As beta-lactam antibiotics inhibit proper cell wall synthesis, faster growing cells have higher potential to accumulate damage, leading to a higher likelihood of death [52–54]. Indeed, robust correlations were found between growth and lysis rates in diverse pairs of beta-lactams and bacteria [52, 58]. Another inherent feature of MSW is high salinity, which results from the high concentrations of solutes (e.g., deliquescent salts) due to water evaporation. High salt concentrations were shown to reduce susceptibility to antibiotics through a cross-protection effect that results from the increased expression of efflux pumps [56, 57]. Finally, the high salinity, ROS, and altered pH in MSW might directly affect the stability and activity of many antibiotic compounds, including beta-lactams [59].

To study wet-dry cycles relevant to natural environments we decided to focus on wet-dry cycles that include an MSW phase. We hypothesized that under such wet-dry cycles, bacteria are less susceptible to antibiotics in comparison to constantly wet (water-saturated) conditions. To test this hypothesis, we quantitatively studied the response of populations of *E. coli*, a well-studied model species for bacterial antibiotic response, to two beta-lactams: Ampicillin (Amp), and Carbenicillin (Crb) (which is a more stable beta-lactam). To this end, we build upon an experimental system developed in our lab that enables us to culture bacteria in wet-dry cycles with an MSW phase, and to quantitatively estimate killing rates and cell survival based on direct CFU counts. We compared the survival of *E. coli* K-12 exposed to differing doses of two common beta-lactam antibiotics in wet-dry cycles with its survival under constantly wet conditions. We further employed computational models, based on our experimental inputs, to elucidate the mechanisms underlying the observed antibiotic response, to be able to achieve a mechanistic understanding of antibiotic response under wet-dry cycles.

METHODS

Strains, media, chemicals, and growth conditions

E. coli DH5α strain was transformed with a plasmid encoding a gene for blue fluorescent protein (BFP2) obtained from Mitja Remus-Emsermann (University of Canterbury Christchurch, NZ) via Addgene (plasmid #118492). In all experiments, a starter culture was grown overnight in M9 0.5X (M9 Minimal Salts Base 5x, Formedium, UK) supplemented with LB 1% (LB Lennox broth, Formedium, UK) and Glucose 20 mM, under agitation set at 220 rpm, at 37 °C. Antibiotics used in the experiments were Amp (Amp sodium salt, Sigma) and Crb (Crb disodium, Formedium, UK). Experiments with other strains included *E. coli* MG1655 and *Pantoea agglomerans* 299R. For the estimation of CFU counts after 17.5 h treatment with various antibiotics in wet-dry cycles and under constantly wet conditions, the following antibiotics were used: Polymixin B sulfate salt (Sigma), Trimethoprim (Sigma), Chloramphenicol (BioPrep), Neomycin (Sigma), Gentamycin (BioPrep), Norfloxacin (Sigma), Ciprofloxacin (Sigma), and Ofloxacin (Sigma).

MIC determination

Overall, 50 µl of an overnight *E. coli* DH5α culture was transferred into 3 ml of fresh medium and incubated for an additional ~3 h until OD_{600} reached a value of ~0.3 (1 cm optical path length). Cells were diluted into 96 microtiter plate (final $OD_{600} = 0.005$) set with a twofold serial dilution of Amp or Crb (Ten serial dilutions from 100 to 0.2 µg/ml) and a control without antibiotics (Eight replicates for each dilution). Plates were incubated for 24 h (at 32 °C), then OD_{600} reads were taken in a plate reader (Synergy H1 Microplate Reader, BioTek Instruments, USA).

Drying-rewetting experiments

Preparation. Overall, 50 µl of *E. coli* DH5α overnight culture were transferred into 3 ml of fresh medium, and incubated for an additional ~3 h until OD_{600} reached a value of ~0.3 (1 cm optical path length). The $OD_{600} = 0.3$ culture was diluted to $OD_{600} = 0.04$ with fresh medium (as a control) or fresh medium supplemented with: (1) 5 µg/ml of Amp or Crb for the 2X MIC experiment (2), 50 µg/ml of Amp or Crb for the 20X MIC experiment.

Wet-dry cycles and constantly wet conditions experimental setup. For the wet-dry cycle experiment, a 1 µl drop from each sample was deposited on the center of a well of a glass-bottom 24-well plate (24-well glass-bottom plate #1.5 high-performance cover glass—Cellvis, USA). A total of six repeats (e.g., drops) was used for the 2X MIC and control experiments, and three repeats for the 20X MIC experiments. The 24-well plate was placed (with the plate lid off) inside a stage-top environmental control chamber (H301-K-FRAME, Okolab srl, Italy) pre equilibrated to 32 °C, 70% RH. For the constantly wet experiment, a volume of 200 µl from each condition (two duplicates) was transferred to separate wells in a glass-bottom 96-well plate (96-well glass-bottom plate #1.5 high-performance cover glass—Cellvis, USA), and placed, with the plate lid on, in an incubator set to 32 °C.

Gradual rewetting protocol. At time $t = 0$, $t = 3$, and $t = 14$ h (times refers to the time that passed from deposition of the drops on the surface of the well), the empty cavities between the wells were filled with 300 µl of H_2O, and the lid was placed on the plate and sealed with tape. The sealed plate was incubated for 90 min at 25 °C (with RH raising to >95% inside the plate). By the end of this step, the dried droplets (MSW) adsorbed water from the humidified air by condensation and deliquescence. At this point, 1 µl samples were pipetted out from the parallel 'constantly wet' experiment and deposited on a second 24-well plate, creating two identical sets of 24-well plates originating from (1) dry conditions (2)

Table 1. Estimated CFU counts after 17.5 h treatment with various antibiotics in wet-dry cycle and constantly wet conditions.

Antibiotics	Class	Mechanism of action	µg/ml	MIC	Wet-Dry cycle (CFU/µl)		Constantly wet (CFU/µl)
Polymyxin B	Polymyxins	Cell membrane	2.5	x2	0	=	0
Trimethoprim	Sulfonamides	Folic acid synthesis inhibitors	**2.5**	**x2**	**10^2**	**>**	**10^1**
			25	**x20**	**10^2**	**>**	**10^1**
Chloramphenicol	Chloramphenicol	Protein synthesis inhibitors	10	x2	10^1	<	10^2
Neomycin	Aminoglycoside		**2.5**	**x2**	**10^2**	**»**	**1–10^1**
			25	x20	0	=	0
Gentamicin			2.5	x2	0	<	10^1
Norfloxacin	Fluoroquinolones	DNA synthesis inhibitors	0.625	x2	10^2	<	10^2–10^3
			12.5	**x20**	**10^2**	**>**	**10^1**
Ciprofloxacin			1.25	x2	0	=	0
Ofloxacin			**0.2**	**x2**	**10^2**	**»**	**0**
			2	x20	0	=	0
Without antibiotics			0	0	10^2–10^3	«	10^5

E.coli DH5α cells were exposed to a range of antibiotics covering a wide spectrum of classes and mechanisms of action. Experiments were performed in the wet-dry cycle and constantly wet modes (long cycle, see Supplementary Fig. S1 as described in 'Methods' section). At the end of the exposure time (17.5 h), agarose pads were overlaid on the samples and incubated at 32 °C for 24 h. The number of CFUs per treatment was estimated by eye inspection of microscopic images that cover the entire area of the agarose pad (13 mm diameter). Each treatment included at least two replicates.

'constantly wet' experiment. Next, 2 µl of fresh medium supplemented with 8 µM of propidium iodide (propidium iodide solution, Sigma) was added to the droplets of both wet-dry and constantly wet 24-well plates. The plates were left closed in the dark for 90 min, at 25 °C. Finally, 4 µl of fresh medium was added to all rewetted droplets, and the plates were incubated for another 30 min under the same conditions.

Agarose pad overlay (CFU assay). At the end of the rewetting procedure, 2 µl were pipetted out (to avoid spillover from the boundaries of the overlaid agarose pad, see below) from each rewetted droplet and placed on the center of a precut round agarose pad (preparation of agarose pads described below). The remaining volume of the droplet (~5 µl) was overlaid by a second agarose pad (round, 16 mm diameter). Agarose pads were incubated for 6–12 h in a humidified chamber at 25 °C before imaging. 1.5% agarose pads were prepared by dissolving 1.5 g/l of agarose in M9 1X solution. The agarose-M9 solution was heated in a microwave until the agarose completely dissolved and a clear solution was obtained. The solution was cooled down to 55 °C, supplemented with glucose 20 mM, and then poured into 10 × 10 cm petri dishes (~15 ml per dish). The agarose plates were left for 2 h at room temperature, and then round disks of agarose pads were chopped using a 13 mm belt punch (ELORA, DE). Agarose pads' overlay was done by picking an agarose disk using a flat spatula, placing the pad on a flat piston taken from a 10 ml syringe, and then carefully lowering the piston toward the rewetted droplet until contact between the pad and the glass surface was made. At this stage, the piston was pulled out while the agarose pad remained attached to the glass surface.

The experiments with *E. coli* MG1655 and *P. agglomerans* were performed as described above with two modifications: (1) the initial volume of the inoculated drop was 2 µl, (2) incubation during the wet-dry cycle was performed in a sealed plastic box that contained an open vessel with 100 ml of near-saturated NaCl solution adjusted to maintain 70 ± 2% RH. The box was placed in an incubator to maintain 32 °C during the experiment.

Microscopy

24-well plates were mounted on a stage top without warming (at room temperature, 25 °C) during image acquisition. Microscopic inspection and image acquisition were performed using an Eclipse Ti-E inverted microscope (Nikon) equipped with Plan Apo 20x/075 N.A. air objective and the Perfect Focus System for maintenance of focus. A LED light source (SOLA SE II, Lumencor) was used for fluorescence excitation. BFP fluorescence was excited with a 395/25 filter, and emission was collected with a T400lp dichroic mirror and a 460/50 filter. Propidium iodide fluorescence was excited with a 560/40 filter, and emission was collected with a T585lpxr dichroic mirror and a 630/75 filter (filters and dichroic mirror from Chroma, USA). A motorized encoded scanning stage (Märzhäuser Wetzlar, DE) was used to collect multiple stage positions. The entire surface of each drop was imaged at the end of the drying phase (BF and BFP channels) and after the addition of propidium iodide (BFP and RFP channels). In these images, 6 × 6 adjacent fields of view (with a 5% overlap) were scanned (3.83 × 3.83 mm). Agarose pads were imaged by scanning 20 × 20 adjacent fields of view (with a 5% overlap) (1.27 × 1.27 cm) in the BFP channel (for the experiments with *E. coli* MG1655 and *P. agglomerans* 299R bright field was used instead of BFP). Images were acquired with an SCMOS camera (ZYLA 19 4.2PLUS, Andor, Oxford Instruments, UK). NIS Elements 5.02 software was used for acquisition.

Image analysis

Image processing. Image processing and analyses were performed to quantify the amount of live (live/dead assay) and viable cells (CFU counts) in each experiment. Preprocessing of all images (i.e., background correction and threshold calibrations) was done in NIS Elements 5.02. For the live cell count within the drops, BFP and PI fluorescence channels of images were thresholded, and the resulting masks were united. Each cell in the unified mask was classified as a live cell if the fraction of its pixels marked with PI was lower than 10%. For the CFU count, BFP channel was thresholded to produce a mask. Only objects with an area larger than 12 µm^2 (~3 cells under our experimental conditions) were counted as CFUs. In some images, in particular in the 'constantly wet' experiments with high antibiotic concentrations, there were a few very large cells that had not divided. Manual inspection and correction was performed to avoid counting these large cells as CFUs.

Estimating growth and lysis rates under various M9 concentrations

Growth and lysis rates were determined following Lee et al. [58] with slight modifications. Overall, 50 µl of an overnight *E. coli* DH5α culture was transferred into 3 ml of fresh medium and incubated for an additional ~3 h until OD_{600} reached a value of ~0.3 (1 cm optical path length). Cells were diluted into 96 microwell plates (final $OD_{600} = 0.005$) with a series of M9 concentrations of: 0.5X, 1X, 2.5X, 5X, 7.5X, 10X, and 15X (supplemented with LB 1% and glucose 20 mM). The plate was incubated in the plate reader for 4.5 h (32°C, without shaking) and OD_{600} was monitored at intervals of 10 min. At time $t \approx 4.5$ h, the plate was pulled out, antibiotic (Amp or Crb) was added to the wells to give a final concertation of 50 µg/ml (equivalent to 20X MIC), and then transferred back to the plate reader for 20 h with an OD_{600} scan every 10 min. Experiments were conducted in 3–5 replicates for each M9 concentration, and repeated three times with similar results. For the M9 10X and 15X experiments, bacteria were incubated for 24 h in the tested M9 concentration to allow for cell acclimation prior to the addition of antibiotics.

Plate reader growth curve analyses. Plate reader readouts were analyzed as follows: First, the background value was subtracted from the OD values. Growth rates in absence of antibiotics were obtained by manual selection of a 2–3 h duration in the log phase (typically between $t = 5$ h to $t = 7$ h) from the experiments without antibiotics (controls), and calculation of the slope. To estimate the lysis rates, we applied Gaussian weighing of adjacent readings (+10 and −10 min) to smooth the OD data, and then found the minimal rate of instantaneous change that occurs after antibiotic addition (i.e., at times > ~6 h). The lysis rate was then estimated by substituting the growth rate without antibiotic, under the relevant control conditions from the minimal actual OD rate of change. The number of repetitions for each data point was five, except for three M9 concentrations (0, 5, and 7.5) in which there were three repeats for the control treatments, and four repeats for the antibiotic treatment.

Computational model of antibiotic response

In this study, we developed an ODE model that describes antibiotic response of bacterial population under wet-dry cycles with an MSW phase. The model describes the dynamics of the following variables: number of live bacterial cells (P), water volume (V) [μl], and active antibiotic content by mass within the system (A) (normalized by [MIC × 1 μl]). The salt content by mass within the system (S_0) (normalized by [Standard M9 concentration × 1 μl]) was constant throughout the simulation.

The external conditions are represented by the amount of imposed water volume at equilibrium $V_{eq}(t)$ [μl]. During the wet-dry-wet cycle, $V_{eq}(t)$ switches from V_{eq-wet} to V_{eq-dry} and from V_{eq-dry} to V_{eq-wet} at times $t_{W\to D}$and $t_{D\to W}$, respectively.

Under the above assumptions, we formulate the following ODE equation system:

$$\frac{dP}{dt} = \left[\left(g\left(\frac{S_0}{V}\right) + d_{stat}\left(\frac{S_0}{V}, \frac{A}{V}\right)\right) \cdot r_{lag}(t) + d_{dyn}\left(\frac{S_0}{V}\right)\right] \cdot P \quad (1)$$

$$\frac{dA}{dt} = d_A\left(\frac{S_0}{V}\right) \cdot A \quad (2)$$

$$\frac{dV}{dt} = r_w \cdot sign\left(V - V_{eq}(t)\right) \quad (3)$$

Where $g(c_S)$ is growth rate, $d_{stat}(c_S, c_A)$ is death rate due to the instantaneous state. $\frac{S_0}{V}$ is the current salt concentration (c_S) and $\frac{A}{V}$ is the current antibiotic concentration (c_A). $r_{lag}(t)$ is lag occurring after the MSW phase, $d_{dyn}(c_S)$ is death rate due to the transition between wet and dry states, $d_A(c_S)$ is the rate of reduction in antibiotic activity, and r_w is the evaporation rate.

A more detailed description of the model is given in Section 1 of the Supporting Information.

Measuring antibiotic stability

See Section 2 of the Supporting Information

Statistical analyses

Comparisons of cell viability (CFU counts) between conditions (wet-dry cycles and the corresponding constantly wet conditions) were performed by Welch t-test. The number of repetitions for each data point in the constantly wet and wet-dry cycles experiments was six repeats for control experiments (low antibiotics), six repeats for low initial antibiotic concentrations (2X MIC), and three repeats for high initial antibiotics concentrations (20X MIC). In the experiments with *E. coli* MG1655 and *P. agglomerans* 299R, the constantly wet experiments included four repeats for each point, and the wet-dry experiments had two repeats.

RESULTS

Experimental system to study bacterial response to antibiotics under wet-dry cycles

To assess the survival of *E. coli* in response to exposure to beta-lactams under wet-dry cycles, we built upon a microscopy-based experimental system that enabled us to study bacteria under varying hydration conditions and MSW [31]. Our wet-dry cycle experiments consisted of three sequential phases: drying, MSW, and rewetting (Fig. 2A; Supplementary Fig. S1). Briefly, *E. coli* DH5α cells were loaded into 1 μl drops of M9 minimal media supplemented with Amp or Crb in concentrations of 5 μg/ml (2X MIC), 50 μg/ml (20X MIC), or without antibiotics. The drops were incubated in an on-stage environmental chamber under constant temperature and RH (32 °C; 70% RH). In about 2 h, the drops dried out, and MSW conditions—in the form of stable thin liquid films—were established. MSW conditions, which constituted the 'dry period', were maintained for either 1 h (short cycle) or 12 h (long cycle) before rewetting. Rewetting was executed by increasing RH followed by the addition of liquid broth medium (see 'Methods' section, Fig. 2A, Supplementary Fig. S1). Corresponding experiments in constantly wet conditions, with equivalent initial cell density, media, and antibiotic concentrations, were conducted likewise (representing continuous water-saturated conditions—see 'Methods' section).

To estimate bacterial survival, we developed a method of counting micro-colonies directly in our experimental system: This was done by laying agarose pads on the colonized surface at the end of the rewetting phase and then, following overnight growth, scanning the surface under the microscope to count micro-colonies (CFU/μl counts—see details in 'Methods' section). As a complementary method for measuring cell survival, we used propidium iodide staining to distinguish between live and dead cells during the rewetting phase (live/dead assays—see 'Methods' section).

Inherent protection from beta-lactams under wet-dry cycles with an MSW phase

Under constantly wet (water-saturated) conditions, there was a rapid killing of most bacteria—consistent with previously reported time kill curves [60]. At 6.5 h, the equivalent time of the short cycle experiment, there was about tenfold reduction in CFU/μl counts for the low antibiotic concentration (2X MIC; less than 10% of the initial cell population were viable) and ~100-fold to 1000-fold reduction of CFU/μl counts for the high antibiotic concentration (20X MIC; 0.1–1% of cells remain viable) (Fig. 2B). After 17.5 h incubation under constantly wet conditions, the equivalent time of the long cycle experiment, there were <10 CFU/μl, representing <0.1% viable cells of the initial cell population, for both antibiotics types and concentrations (Fig. 2B).

Remarkably, in the long wet-dry cycle experiments where cells were exposed to 12 h of MSW, there were >1000 CFU/μl (Fig. 2B), representing at least two orders of magnitude higher CFU than under constantly wet conditions, at the corresponding time ($t =$ 17.5 h) (Fig. 2B) (two-sample t-test, $p < 0.05$). In the short wet-dry cycle experiments, however, we saw either similar CFU counts as under constantly wet conditions at the corresponding time (Amp experiments), or only modest increase in CFU counts (2X MIC Crb experiment, two-sample t-test, $p < 0.05$) (Fig. 2B). Similar trends, though with an order of magnitude smaller differences, were observed by live/dead assays for cell survival rather than CFU counts (Supplementary Figs. S2 and S3).

Inspection of the microscopy images confirmed that the number of cells under constantly wet conditions with antibiotics was indeed much smaller than in the equivalent wet-dry cycle experiment (Fig. 2C, left column; Supplementary Fig. S4), likely because many cells were lysed due to cell wall deterioration and osmotic rupture [61]. Many of the live cells that did survive were longer and thicker, a known effect of beta-lactams (Fig. 2C; Supplementary Figs. S4 and S5) [62]. In contrast, under wet-dry cycles and MSW, while cells were not growing or dividing, most cells were intact, and there were many more live cells than there were under the corresponding constantly wet conditions (Fig. 2C; Supplementary Figs. S4 and S5). High correlation was found between the numbers of live cells and the number of CFUs ($r =$ 0.998, $p < 0.001$, Supplementary Figs. S6 and S7). In addition, micro-colonies could be easily observed on the agarose pads that were placed on the well bottoms (see 'Methods' section), with

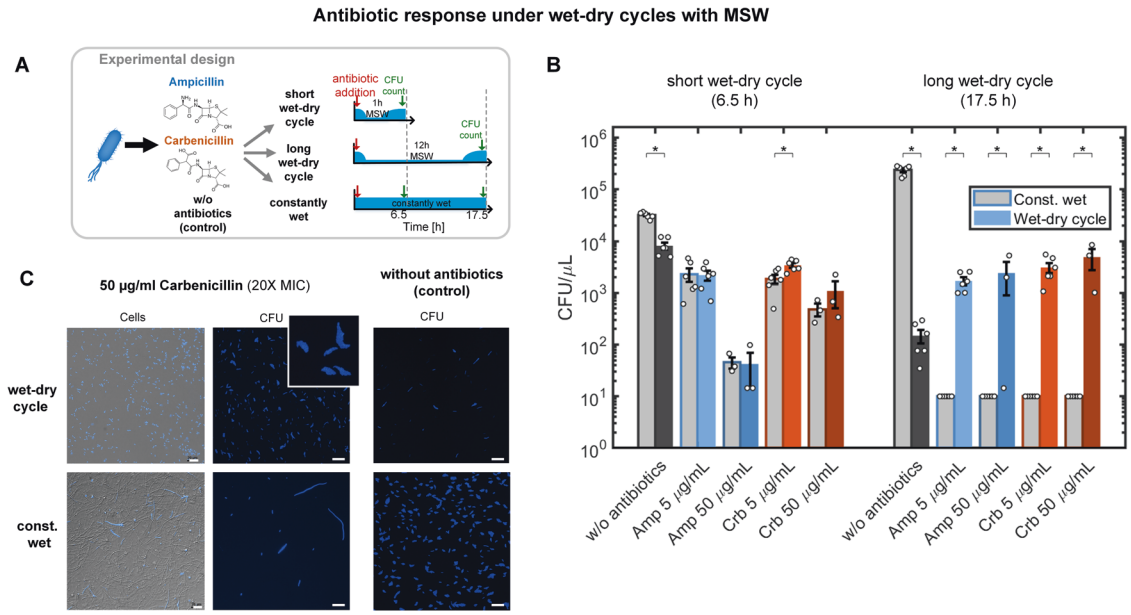

Fig. 2 Wet-dry cycles with MSW protect bacteria from beta-lactam antibiotics. A Experimental setup. *E. coli* cells were exposed to Amp, Crb, or antibiotic-free media and incubated under wet-dry cycles (short or long) or under constantly wet conditions. CFU were counted at the end of the wet-dry cycle or equivalent time from the corresponding constantly wet experiment. **B** Bacterial response to Amp and Crb under short and long wet-dry cycles and under constantly wet conditions. Bars and error bars represent mean ± SE CFU/μl at either 6.5 h (short wet-dry cycle) or 17.5 h (long wet-dry cycle). White circles represent replicates. Amp and Crb were added at concentrations of 2X MIC and 20X MIC; no antibiotic was added in controls. CFU assay was conducted as described in 'Methods' section. Asterisk indicates statistical significance at $p < 0.05$ (pairwise *t*-test). **C** Representative microscopy images from a long wet-dry cycle experiment with Crb (20X MIC) and the corresponding constantly wet experiment (both at $t = 17.5$ h). Left column shows cells morphology and BFP2 expression level during the rewetting phase. Healthy morphology and BFP2 expression were observed under MSW conditions (upper panel) while elongated cells and loss of BFP2 signal were common under constantly wet conditions (lower panel). Middle column shows cell recovery on the agarose pad after overnight incubation (see 'Methods' section). Micro-colonies formed on the agarose pad that was overlaid on the wet-dry cycle experiment, while only few micro-colonies were detected in the equivalent constantly wet experiment. Right column shows cell recovery on the agarose pad after overnight incubation from the control experiments (without antibiotics). Few micro-colonies were found in the long wet-dry cycle experiment due to low survival under MSW conditions (upper panel) in contrast to high survival under constantly wet conditions without antibiotics (lower panel).

significantly more colonies in the long wet-dry cycle experiments than under constantly wet conditions (Fig. 2B, C; Supplementary Fig. S8). Without antibiotics, there were indeed many more CFUs in the constantly wet experiment compared to the wet-dry cycle experiments (Fig. 2C; Supplementary Fig. S8), reflecting high growth and high survival under wet conditions, and slow (or no) growth and lower survival in MSW.

The underlying mechanisms of the observed protection from beta-lactams

To better understand the mechanisms underlying the observed protection, we examined several directions: deactivation of antibiotics under MSW conditions, tolerance by slow growth, and cross protection due to high salt concentrations.

We first sought to assess the stability of both antibiotics during the drying process and under MSW conditions, and test whether a decay in their activity can explain our results. We found that during drying followed by an MSW period, a portion of the antibiotics was deactivated (in particular Amp; less so Crb, Fig. 3A), likely via degradation caused by the high salt concentrations or other physicochemical properties of MSW (Supplementary Fig. S9). The rates of antibiotic deactivation during drying and MSW were not sufficient, however, to explain the observed high cell survival at the end of the long wet-dry cycle, since high concentrations of active antibiotics were retained throughout the duration of the cycle. Moreover, as the concentration of all solutes increases during drying due to water evaporation, the antibiotic concentrations are expected to increase accordingly. In previous work, under similar conditions (medium and RH), we estimated a concentration factor of ~50 times [31]. Thus, by the time MSW is formed, the antibiotic concentration in the experiment that began with 20X MIC is expected to reach ~1000X MIC (assuming most of the antibiotic is still active after 1 h in MSW, Fig. 3A). Even if we assume that only 10% of the antibiotic remains active at the end of a 12 h MSW period, it is not clear how so many cells could survive a high antibiotic dosage of ~100X MIC. Thus, there must be additional mechanisms, other than the decay of antibiotic activity, underlying the observed high bacterial survival.

Next, we sought to test the impact of salt concentrations on lysis rates. Cross protection due to high salt concentrations, which is one major stress associated with MSW, has been previously reported [57]. During drying and formation of MSW, cells are exposed to rapid increase in salt concentration until stable concentrated solutions in the form of microdroplets or thin films are formed (with an estimated final concentration of about M9 ~25X with osmolarity of ~6.7 Osm/L [31]). Adopting a method suggested by Lee et al. [58], we estimated the lysis rates under a range of M9 medium concentrations. We found that at M9 concentrations ≥10X, lysis rates decreased significantly, approaching zero at M9 15X (Fig. 3B). Lysis rates were also highly correlated to cell-growth rates, under the tested M9 concentrations. At high salt concentrations, growth rates were low, as were estimated lysis rates (Fig. 3B; Supplementary Fig. S10), consistent with the well-known correlations between bacterial growth rates and beta-lactams' response [52, 58]. We therefore conclude that the high salinity leads to a pronounced reduction in lysis rates, via cross-protection or tolerance by slow growth, or both. Because high salinity is an inherent property of MSW, it likely plays a major role

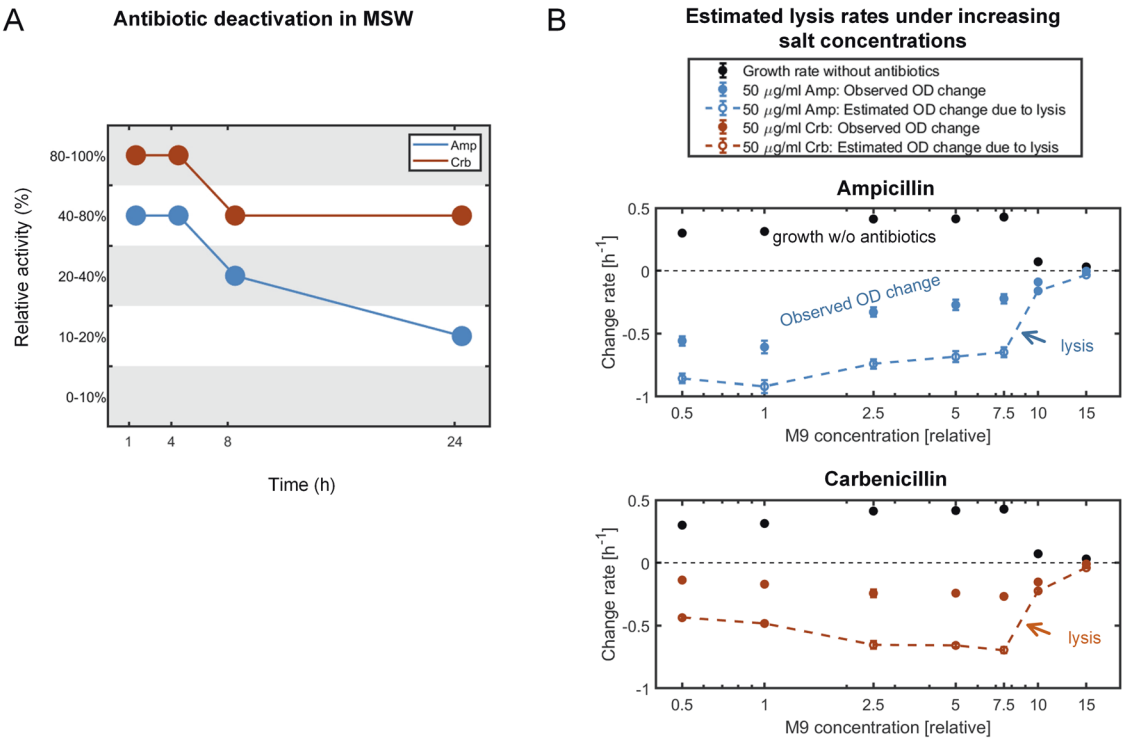

Fig. 3 Antibiotic deactivation in MSW and estimation of growth and lysis rates. A Amp and Crb stability under MSW conditions was estimated as described in 'Methods' section. Amp is deactivated faster than Crb, with a reduction of more than 50% activity after 8 h under MSW conditions. Amp deactivation was more pronounced, with 10–20% remaining activity after 24 h in MSW, compared to 40–80% remaining activity of Crb. This deactivation of antibiotics is explained, at least partially, by the high salt concentrations (Supplementary Fig. S9). **B** Estimation of growth and lysis rates in response to antibiotics under increasingly concentrated M9 medium (see 'Methods' section). 50 μg/ml of beta-lactam antibiotic (Amp or Crb) was added to a mid-exponential growth phase of *E. coli* culture growing in various M9 concentrations. Lysis rates decrease significantly (as reflected by less negative estimated OD change rates due to lysis) from M9 10X, approaching zero lysis at M9 15X.

in the reduced lysis rates that we observed in the longer wet-dry cycle.

Beta-lactams cross-protect bacteria from drying and MSW conditions

Surprisingly, we observed that in the long wet-dry cycle experiment, cell survival was significantly higher in the experiments with antibiotics than they were in the corresponding experiments without antibiotics (Fig. 2B; Supplementary Fig. S2, two-sample *t*-test $p < 0.05$). That is, the addition of antibiotics before drying protected bacteria from stresses associated with drying and MSW conditions, and increased cell survival. Without antibiotics, about 1% of the cells were viable after 12 h in MSW (CFU counts) (Fig. 2B), while more than 10% were viable when antibiotics were added (Fig. 2B). This unexpected result was observed for both Amp and Crb, and at both tested concentrations (Fig. 2B). However, we note that cross-protection was particularly pronounced in these settings, and appears to depend upon the drying and rewetting times (prior to and after MSW). These results point to an additional cross-protection effect that has not been reported before, wherein antibiotics lead to cells' increased protection from stresses associated with drying and MSW.

A computational model provides a mechanistic understanding of experimental results

We then aimed to develop a computational model that, based on our experimental results and their synthesis, can provide a mechanistic understanding of bacterial response to beta-lactams in wet-dry cycles with MSW phase. Toward this goal, we developed a mathematical model—a population-based ODE model—that incorporates the mode of action of the proposed mechanisms underlying increased bacterial protection from antibiotics under wet-dry cycles (see 'Methods' section and Supplementary Information 'Model description'). Briefly, our model assumes that cell-growth rates depend upon salt concentrations (i.e., medium conc.), and death rates depend upon antibiotic response, osmotic stress, and the observed reduced susceptibility to beta-lactams. The model takes into account the decay of antibiotic activity and the changes in water volume during drying and rewetting (Fig. 4A). Most model parameters were extracted from the experimental results (see Supplementary Information 'Model description', Supplementary Figs. S11 and S12). The drying and rewetting dynamics, combined with antibiotic deactivation at high salt concentrations, can be seen as a trajectory in the 'salt concentration × antibiotic concentration' domain that dictates bacterial population dynamic (Fig. 4B). The model suggests how changes in water volumes, salt, and antibiotic concentrations, and the formation of MSW, govern the instantaneous death rate during the various phases (I, II, …,V) of a wet-dry cycle (Fig. 4A), in such a way that the resulting population sizes qualitatively agree with our experiments (Fig. 4D, E; Supplementary Figs. S13, S14, S15). The model demonstrates the role that reciprocal cross-protection plays in the observed results, and how the duration of MSW conditions can affect the dynamics after rewetting, i.e., whether or not antibiotic concentration will inhibit growth (Fig. 4B). Importantly, incorporation of 'tolerance by lag' [18] after rewetting was required to achieve qualitative agreement with the experimental results. 'Tolerance by lag' is the transient protection of cells during the 'lag phase' following a transition between growth arrest and permissive conditions, which in our experiments, correspond to the rewetting phase

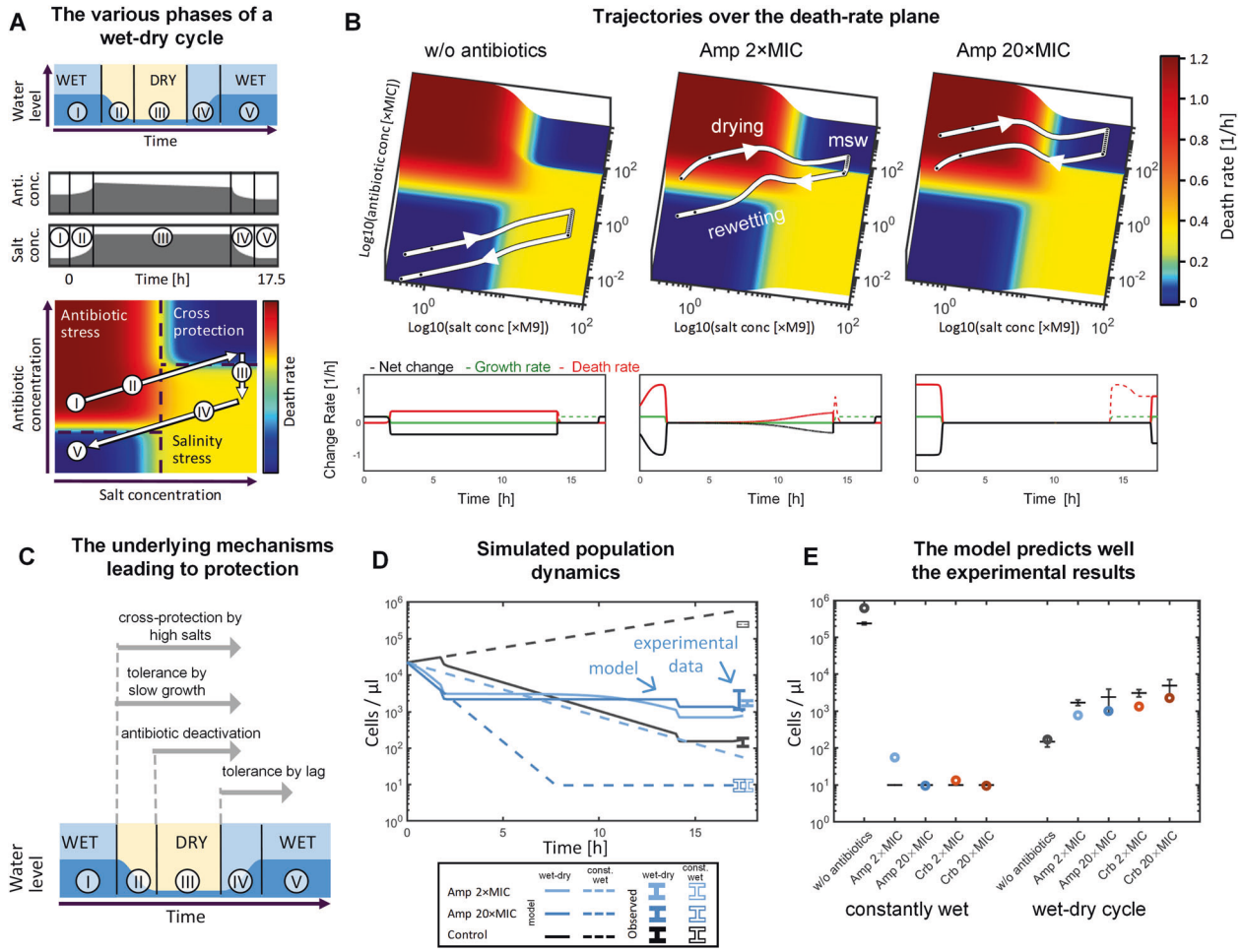

Fig. 4 Mathematical modeling provides a mechanistic understanding of antibiotic response under wet-dry cycles with MSW. A Under wet-dry cycle, varying water volume and antibiotic deactivation rates trace a trajectory on the salt conc. × antibiotic conc. 2D plane (white arrows). The bacterial cell-death rate (see color bar) has four major zones: no-stress zone (low salt – low antibiotics), antibiotic stress (low salts – high antibiotics), salinity stress (high salts – low antibiotics) and a zone of cross protection (high salts – high antibiotics). **B** Examples of the trajectories of various initial antibiotic concentrations, with the resulting bacterial growth and death rates. Differing trajectories result in differing durations of cross-protection. In addition, antibiotic deactivation can lead to traversing the cross protection and returning to a no-stress zone after rewetting **C** Schematic illustration of the mechanisms underlying the observed protection and their time of action during the various phases of a wet-dry cycle. **D** Dynamics of simulations, compared to observed results at the end of the long wet-dry cycle experiment and the corresponding 'constantly wet' experiments. **E** Comparison of simulation results to observed results from a 17.5 h wet-dry cycle and the equivalent 'constantly wet' experiment.

[18] (Fig. 4A,C). The lag phase was reflected in the experiments by a gap between the rewetting time and the initiation of cell divisions, that positively correlated with the duration of MSW conditions (longer lag time of 2–3 h in the long cycle compared to <1 h in the short cycle). As 'tolerance by lag' was necessary to explain the reduced killing after rewetting in the long cycle, the model suggests that such tolerance likely plays a role in reduced overall bacterial susceptibility to beta-lactams, in particular when antibiotic concentrations are high and the 'dry' periods are long.

Protection from beta-lactams under wet-dry cycles is not strain specific

Finally, we asked whether protection from beta-lactams under wet-dry cycles is specific to *E. coli* DH5α, or represents a broader phenomenon. To test this, we repeated the experiments with the wild-type laboratory *E. coli* K-12 strain MG1655 and with *Pantoea agglomerans* (strain 299R)—an environmental bacterial species that is common on leaf and root surfaces and in soil. We tested the response of these strains under increasing Amp concentrations and found similar protection from the antibiotic (Fig. 5). At Amp concentrations ≥5 µg/ml, there were significantly more CFU/µl in wet-dry cycles than there were under constantly wet conditions (two-sample *t*-test, $p < 0.05$). The results of these experiments indicate that the observed protection is neither strain- nor species-specific, and is likely a general phenomenon.

DISCUSSION

In this study, we demonstrated protection of *E. coli* cells from two beta-lactam antibiotics, Amp, and Crb, under wet-dry cycles with an MSW phase. We show that bacteria exposed to high concentrations of antibiotics—considerably higher than the MIC—showed significantly higher survival under a wet-dry cycle with prolonged 'dry' MSW conditions than they did under constantly wet conditions (Fig. 2).

Through a combination of experiments and computational modeling, we were able to point to four mechanisms operating in increased protection from beta-lactams under wet-dry cycles with MSW: (1) cross-protection due to high salt concentrations, (2) 'tolerance by slow growth', (3) deactivation of antibiotics by the physicochemical conditions associated with drying and MSW, and (4) 'tolerance by lag' [18] during rewetting. These mechanisms act

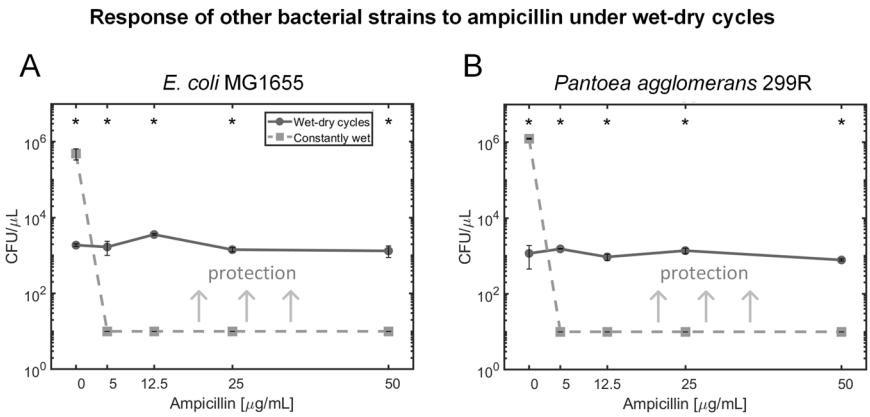

Fig. 5 Antibiotic responses of other strains to Amp. CFU counts at the end of long wet-dry cycles and the equivalent constantly wet conditions (at $t = 17.5$ h). **A** *E. coli* MG1655. **B** *P. agglomerans*. 299R. Shown are mean ± SE CFU/μl ($N = 2$ in wet-dry cycles; $N = 4$ in const. wet conditions); asterisk indicates statistical significance at $p < 0.05$ (pairwise *t*-test). Note that protection is observed for both strains across all tested Amp concentrations.

at various phases of the wet-dry cycle (Fig. 4C). Cross protection due to high salts and 'tolerance by slow growth' act in late drying and during the MSW phase, when antibiotic deactivation occurs. As deactivation is time dependent, the MSW duration modulates the accessible concentration of 'active' antibiotic after rewetting. Finally, the 'tolerance by lag' acts in the rewetting phase. Our computational model enabled us to integrate the operation of these four mechanisms, and to analyze the effect of each mechanism, and its associated parameters, on the overall population response to antibiotics under wet-dry cycles.

It is difficult to assess the exact contribution of each of the first two mechanisms, i.e., cross protection due to high salts, and the 'tolerance by slow growth'. This is partly due to the fact that activation of stress response mechanisms (e.g., from high salinity) that provides cross-protection from antibiotics, is intertwined with slow growth, which is known to lead to 'tolerance by slow growth' [18]. While our experiments indicate that high salt concentrations are a major stress factor that induces cross protection (Fig. 3B), other stresses associated with drying and MSW, such as altered pH and ROS, may be involved as well. Finally, we demonstrated that the deactivation of the antibiotics was not enough to explain the observed protection. We note that we could not rule out the possibility that reduced bio-accessibility of antibiotics under MSW conditions played a role in this protection.

Identifying the molecular mechanism associated with the observed tolerance was not the focus of the current study, but rather aiming at a mechanistic understanding of the population-level response to antibiotics under wet-dry cycles and MSW. Possible molecular mechanisms facilitating reduced susceptibility associated with drying, rewetting, and MSW may include: expression of efflux pumps, general stress response and RpoS, oxidative stress response, reduced energy metabolism, SOS response, (p)ppGpp signaling, and toxin-antitoxin modules [23, 63–67]. Further research is required to identify the molecular mechanisms that facilitate the observed protection from beta-lactams under wet-dry cycles.

A surprising result was the significantly increased cross-protection from drying and MSW by the presence of lethal doses of antibiotics before drying. Although evidence for cross-protection by antibiotics on other stresses, including osmotic stress in particular, has been reported, it was associated with resistant mutant strains, and not due to induced tolerance [68]. Thus, substantial increased bacterial survival under MSW is, to the best of our knowledge, novel. Our experiments suggest that this cross-protection depends upon the drying times and the killing kinetics during drying: If drying is rapid, death from osmotic shock will be the dominant factor; if drying is slow, lysis from long exposure to antibiotics will dictate the survival rates. Our model predicts that such cross-protection can occur in intermediate drying times. Further research is required to thoroughly test this prediction. As cross-protection could be substantial—as observed in our experiments—showing even approximately tenfold higher survival under wet-dry cycles if antibiotics are added (Fig. 2), this is worth further investigation. Such a pronounced cross-protection might have significant implications for how we perceive antibiotics in the microbial world. For example, secretion of antibiotics may actually function to protect neighboring co-occurring species from drying, rather than killing them.

Our computational model was developed in order to achieve a population-level mechanistic understanding of bacterial response to beta-lactam antibiotics in wet-dry cycles. It thus aimed to validate that the proposed underlying mechanisms obtained from our experiments are sufficient to produce results that agree, at least qualitatively, with the experimental data. The model is relatively simple, and does not take into account the heterogeneity of individual cells within populations, nor the microscale heterogeneity of hydration and physicochemical conditions [31]. Yet the model highlights the mechanisms suggested as underlying the observed increased protection, and clarify their specific role in the response. The two-variable death rate function (Fig. 4B) is a key component of the model that provides a concise link between water level, salt and antibiotic concentration, and death rates. Accordingly, the trajectory on this death rate plane during a wet-dry cycle was illuminating. The model explains why a longer MSW phase may increase protection, as seen for the higher Amp concentrations. This is due to extended antibiotic deactivation and a longer lag phase, which extends the 'tolerance by lag' period that protects from remaining antibiotics after rewetting (see also Supplementary Fig. S13). In general, the model can be used to predict response to antibiotics and overall survival under various scenarios of hydration dynamics, initial antibiotic concentrations, and wet-dry cycle durations (Supplementary Figs. S15 and S16). Additional or alternative mechanisms, or their details, are possible. For example, it was not clear whether the increased cross-protection from MSW stresses facilitated by the antibiotics depends upon the antibiotic concentration prior to drying, or the instantaneous one while under MSW. Further work is required to extend and refine the model, including additional experimental work to cover other antibiotics, additional bacterial strains, and a wider range of parameters.

In this work, we chose to focus on beta-lactams and the model bacterium *E. coli*. Preliminary results of a wider set of experiments that we conducted, point to increased protection of wet-dry cycles against various major antibiotic classes that inhibit DNA

replication (Fluoroquinolones) and synthesis (e.g., Trimethoprim), and antibiotics that inhibit protein synthesis (Aminoglycosides) (Table 1). 'Tolerance by slow growth' and reduced metabolism is a general mechanism that has been demonstrated in these antibiotic families [52–54], supporting our expectations for increased protection under wet-dry cycles. Cross-protection via increased expression of efflux pumps, is a mechanism that has been demonstrated to reduce susceptibility to antibiotics of various families [57, 65], and depends upon chemical properties of the antibiotic (e.g., hydrophobicity). Also, as stability of various antimicrobial compounds may vary significantly, their degradation or deactivation under MSW may vary as well. Moreover, the present study did not explore antibiotic response of mature biofilms that may confirm tolerance due to matrix properties. Further research is thus required to assess the protection levels to other antibiotics, to investigate their underlying mechanisms, and to extend the study to other bacterial species.

This work brings a new perspective on how we understand bacterial response to major classes of antibiotics in several globally important microbial ecosystems, including the largest terrestrial microbial habitats: soil, rock surfaces, and plant root and leaf surfaces. It is also likely important to indoor environments, most of which are exposed to recurring wet-dry cycles with MSW, and of relevance to human skin microbiome. We demonstrate that under wet-dry cycles, bacterial response to major antibiotics classes is very different than it is under constantly wet conditions. Indeed, under wet-dry cycles with 'dry' MSW conditions, concentrations much higher than the clinical MIC of these antibiotics are not very effective at killing bacteria. These findings have broad implications on the way we understand the role of antibiotics in microbial warfare and interspecies competition. As tolerance has been shown to boost the emergence of resistance [69, 70], the inherent tolerance under wet-dry cycles might also facilitate the evolution of antibiotic resistance.

REFERENCES

1. Or D, Smets BF, Wraith J, Dechesne A, Friedman S. Physical constraints affecting bacterial habitats and activity in unsaturated porous media–a review. Adv Water Resour. 2007;30:1505–27.
2. Burkhardt J, Hunsche M. "Breath figures" on leaf surfaces—formation and effects of microscopic leaf wetness. Front plant Sci. 2013;4:422.
3. Wolf AB, Vos M, de Boer W, Kowalchuk GA. Impact of matric potential and pore size distribution on growth dynamics of filamentous and non-filamentous soil bacteria. PloS One. 2013;8:e83661.
4. Forsberg KJ, Reyes A, Wang B, Selleck EM, Sommer MO, Dantas G. The shared antibiotic resistome of soil bacteria and human pathogens. Science. 2012;337:1107–11.
5. Williams S, Vickers J. The ecology of antibiotic production. Microb Ecol. 1986;12:43–52.
6. Raaijmakers JM, Weller DM, Thomashow LS. Frequency of antibiotic-producing Pseudomonas spp. in natural environments. Appl Environ Microbiol. 1997;63:881–7.
7. Wells JS, Hunter JC, Astle GL, Sherwood JC, Ricca cM, Trejo WH, et al. Distribution of β-lactam and β-lactone producing bacteria in nature. The. J Antibiot. 1982;35:814–21.
8. Kinkel LL, Schlatter DC, Xiao K, Baines AD. Sympatric inhibition and niche differentiation suggest alternative coevolutionary trajectories among Streptomycetes. ISME J. 2014;8:249–56.
9. Vetsigian K, Jajoo R, Kishony R. Structure and evolution of Streptomyces interaction networks in soil and in silico. PLoS Biol. 2011;9:e1001184.
10. Traxler MF, Kolter R. Natural products in soil microbe interactions and evolution. Nat Prod Rep. 2015;32:956–70.
11. Franklin AM, Aga DS, Cytryn E, Durso LM, McLain JE, Pruden A, et al. Antibiotics in agroecosystems: introduction to the special section. J Environ Qual. 2016;45:377–93.
12. Jechalke S, Heuer H, Siemens J, Amelung W, Smalla K. Fate and effects of veterinary antibiotics in soil. Trends Microbiol. 2014;22:536–45.
13. Mompelat S, Le Bot B, Thomas O. Occurrence and fate of pharmaceutical products and by-products, from resource to drinking water. Environ Int. 2009;35:803–14.
14. Kelsic ED, Zhao J, Vetsigian K, Kishony R. Counteraction of antibiotic production and degradation stabilizes microbial communities. Nature. 2015;521:516–9.
15. Cordero OX, Wildschutte H, Kirkup B, Proehl S, Ngo L, Hussain F, et al. Ecological populations of bacteria act as socially cohesive units of antibiotic production and resistance. Science. 2012;337:1228–31.
16. Schlatter DC, Song Z, Vaz-Jauri P, Kinkel LL. Inhibitory interaction networks among coevolved Streptomyces populations from prairie soils. Plos One. 2019;14:e0223779.
17. Abrudan MI, Smakman F, Grimbergen AJ, Westhoff S, Miller EL, Van Wezel GP, et al. Socially mediated induction and suppression of antibiosis during bacterial coexistence. Proc Natl Acad Sci. 2015;112:11054–9.
18. Brauner A, Fridman O, Gefen O, Balaban NQ. Distinguishing between resistance, tolerance and persistence to antibiotic treatment. Nat Rev Microbiol. 2016;14:320.
19. Andersson DI, Levin BR. The biological cost of antibiotic resistance. Curr Opin Microbiol. 1999;2:489–93.
20. Handwerger S, Tomasz A. Antibiotic tolerance among clinical isolates of bacteria. Annu Rev Pharmacol Toxicol. 1985;25:349–80.
21. Kester JC, Fortune SM. Persisters and beyond: mechanisms of phenotypic drug resistance and drug tolerance in bacteria. Crit Rev Biochem Mol Biol. 2014;49:91–101.
22. Wood KB, Cluzel P. Trade-offs between drug toxicity and benefit in the multi-antibiotic resistance system underlie optimal growth of E. coli. BMC Syst Biol. 2012;6:1–11.
23. Nguyen D, Joshi-Datar A, Lepine F, Bauerle E, Olakanmi O, Beer K, et al. Active starvation responses mediate antibiotic tolerance in biofilms and nutrient-limited bacteria. Science. 2011;334:982–6.
24. Meredith HR, Srimani JK, Lee AJ, Lopatkin AJ, You L. Collective antibiotic tolerance: mechanisms, dynamics and intervention. Nat Chem Biol. 2015;11:182.
25. Nagarajan R, Boeck LD, Gorman M, Hamill RL, Higgens CE, Hoehn MM, et al. beta.-Lactam antibiotics from Streptomyces. J Am Chem Soc. 1971;93:2308–10.
26. Imada A, Kitano K, Kintaka K, Muroi M, Asai M. Sulfazecin and isosulfazecin, novel β-lactam antibiotics of bacterial origin. Nature. 1981;289:590–1.
27. Sykes R, Cimarusti C, Bonner D, Bush K, Floyd D, Georgopapadakou N, et al. Monocyclic β-lactam antibiotics produced by bacteria. Nature. 1981;291:489.
28. Wells JS, TREJO WH, PRINCIPE PA, Bush K, Georgopapadakou N, Bonner DP, et al. EM5400, a family of monobactam antibiotics produced by Agrobacterium radiobacter. J Antibiot. 1982;35:295–9.
29. ThaKurla B, Lahon K. The beta lactam antibiotics as an empirical therapy in a developing country: An update on their current status and recommendations to counter the resistance against them. J Clin Diagn Res. 2013;7:1207.
30. Russ D, Glaser F, Tamar ES, Yelin I, Baym M, Kelsic ED, et al. Escape mutations circumvent a tradeoff between resistance to a beta-lactam and resistance to a beta-lactamase inhibitor. Nat Commun. 2020;11:1–9.
31. Grinberg M, Orevi T, Steinberg S, Kashtan N. Bacterial survival in microscopic surface wetness. eLife. 2019;8:e48508.
32. Orevi T, Kashtan N. Life in a droplet: microbial ecology in microscopic surface wetness. Front Microbiol. 2021;12:797.
33. Mauer LJ, Taylor LS. Water-solids interactions: deliquescence. Annu Rev food Sci Technol. 2010;1:41–63.
34. Wise ME, Martin ST, Russell LM, Buseck PR. Water uptake by NaCl particles prior to deliquescence and the phase rule. Aerosol Sci Technol. 2008;42:281–94.
35. Burkhardt J, Koch K, Kaiser H. Deliquescence of deposited atmospheric particles on leaf surfaces. J Water, Air Soil Pollut: Focus. 2001;1:313–21.
36. Beattie GA. Water relations in the Interaction of foliar bacterial pathogens with plants. Annu Rev Phytopathol. 2011;49:533–55.
37. Davila AF, Hawes I, Ascaso C, Wierzchos J. Salt deliquescence drives photosynthesis in the hyperarid A tacama D esert. Environ Microbiol Rep. 2013;5:583–7.
38. Dai S, Shin H, Santamarina JC. Formation and development of salt crusts on soil surfaces. Acta Geotechnica. 2016;11:1103–9.
39. Trechsel HR. Moisture control in buildings. ASTM International; West Conshohocken, PA19428-2959, USA; 1994.
40. Schwartz-Narbonne H, Donaldson DJ. Water uptake by indoor surface films. Sci Rep. 2019;9:1–10.
41. Patrick D, Findon G, Miller T. Residual moisture determines the level of touch-contact-associated bacterial transfer following hand washing. Epidemiol Infect. 1997;119:319–25.
42. Tang IN, Munkelwitz HR. Composition and temperature dependence of the deliquescence properties of hygroscopic aerosols. Atmos Environ Part A Gen Top. 1993;27:467–73.
43. Pöschl U. Atmospheric aerosols: composition, transformation, climate and health effects. Angew Chem Int Ed. 2005;44:7520–40.
44. Tecon R. Bacterial survival: life on a leaf. eLife. 2019;8:e52123.
45. Vejerano EP, Marr LC. Physico-chemical characteristics of evaporating respiratory fluid droplets. J R Soc Interface. 2018;15:20170939.

46. Rubasinghege G, Grassian VH. Role (s) of adsorbed water in the surface chemistry of environmental interfaces. Chem Commun. 2013;49:3071–94.
47. Campbell TD, Febrian R, McCarthy JT, Kleinschmidt HE, Forsythe JG, Bracher PJ. Prebiotic condensation through wet–dry cycling regulated by deliquescence. Nat Commun. 2019;10:1–7.
48. Alsved M, Holm S, Christiansen S, Smidt M, Rosati B, Ling M, et al. Effect of aerosolization and drying on the viability of pseudomonas syringae cells. Front Microbiol. 2018;9:3086.
49. Xie X, Li Y, Zhang T, Fang HH. Bacterial survival in evaporating deposited droplets on a teflon-coated surface. Appl Microbiol Biotechnol. 2006;73:703–12.
50. Runkel S, Wells HC, Rowley G. Living with stress: a lesson from the enteric pathogen Salmonella enterica. Adv Appl Microbiol. 2013;83:87–144.
51. Amaeze N, Akinbobola A, Chukwuemeka V, Abalkhaila A, Ramage G, Kean R, et al. Development of a high throughput and low cost model for the study of semi-dry biofilms. Biofouling. 2020:36:403–15.
52. Tuomanen E, Cozens R, Tosch W, Zak O, Tomasz A. The rate of killing of Escherichia coli byβ-lactam antibiotics is strictly proportional to the rate of bacterial growth. Microbiology. 1986;132:1297–304.
53. Eng R, Padberg F, Smith S, Tan E, Cherubin C. Bactericidal effects of antibiotics on slowly growing and nongrowing bacteria. Antimicrobial Agents Chemother. 1991;35:1824–8.
54. Lee S, Foley E, Epstein JA. Mode of action of penicillin: I. Bacterial growth and penicillin activity—Staphylococcus aureus FDA. J Bacteriol. 1944;48:393.
55. Lopatkin AJ, Stokes JM, Zheng EJ, Yang JH, Takahashi MK, You L, et al. Bacterial metabolic state more accurately predicts antibiotic lethality than growth rate. Nat Microbiol. 2019;4:2109–17.
56. Yoon H, Park B-Y, Oh M-H, Choi K-H, Yoon Y. Effect of NaCl on heat resistance, antibiotic susceptibility, and Caco-2 cell invasion of Salmonella. BioMed Res Int. 2013;2013:274096.
57. Zhu M, Dai X. High salt cross-protects Escherichia coli from antibiotic treatment through increasing efflux pump expression. mSphere 3: e00095-18. mSphere. 2018;3:e00095–18.
58. Lee AJ, Wang S, Meredith HR, Zhuang B, Dai Z, You L. Robust, linear correlations between growth rates and β-lactam–mediated lysis rates. Proc Natl Acad Sci. 2018;115:4069–74.
59. Loftin KA, Adams CD, Meyer MT, Surampalli R. Effects of ionic strength, temperature, and pH on degradation of selected antibiotics. J Environ Qual. 2008;37:378–86.
60. Thonus IP, Fontijne P, Michel MF. Ampicillin susceptibility and ampicillin-induced killing rate of Escherichia coli. Antimicrobial Agents Chemother. 1982;22:386–90.
61. Cho H, Uehara T, Bernhardt TG. Beta-lactam antibiotics induce a lethal malfunctioning of the bacterial cell wall synthesis machinery. Cell. 2014;159:1300–11.
62. Yao Z, Kahne D, Kishony R. Distinct single-cell morphological dynamics under beta-lactam antibiotics. Mol Cell. 2012;48:705–12.
63. Battesti A, Majdalani N, Gottesman S. The RpoS-mediated general stress response in Escherichia coli. Annu Rev Microbiol. 2011;65:189–213.
64. Bernier SP, Lebeaux D, DeFrancesco AS, Valomon A, Soubigou G, Coppée J-Y, et al. Starvation, together with the SOS response, mediates high biofilm-specific tolerance to the fluoroquinolone ofloxacin. PLoS Genet. 2013;9:e1003144.
65. Pu Y, Zhao Z, Li Y, Zou J, Ma Q, Zhao Y, et al. Enhanced efflux activity facilitates drug tolerance in dormant bacterial cells. Mol Cell. 2016;62:284–94.
66. Martins D, McKay G, Sampathkumar G, Khakimova M, English AM, Nguyen D. Superoxide dismutase activity confers (p) ppGpp-mediated antibiotic tolerance to stationary-phase Pseudomonas aeruginosa. Proc Natl Acad Sci. 2018;115:9797–802.
67. Page R, Peti W. Toxin-antitoxin systems in bacterial growth arrest and persistence. Nat Chem Biol. 2016;12:208–14.
68. Liao X, Ma Y, Daliri EB-M, Koseki S, Wei S, Liu D, et al. Interplay of antibiotic resistance and food-associated stress tolerance in foodborne pathogens. Trends Food Sci Technol. 2020;95:97–106.
69. Levin-Reisman I, Brauner A, Ronin I, Balaban NQ. Epistasis between antibiotic tolerance, persistence, and resistance mutations. Proc Natl Acad Sci. 2019;116:14734–9.
70. Levin-Reisman I, Ronin I, Gefen O, Braniss I, Shoresh N, Balaban NQ. Antibiotic tolerance facilitates the evolution of resistance. Science. 2017;355:826–30.

ACKNOWLEDGEMENTS

We thank Jonathan Friedman, Nathalie Balaban, Yael Helman, and Yitzhak Hadar for valuable comments and discussions. *P. agglomerans* 299R was kindly provided by Steve E. Lindow. NK is supported by research grants from the James S. McDonnell Foundation (Studying Complex Systems Scholar Award, Grant #220020475) and from the Israel Science Foundation (ISF #1396/19).

AUTHOR CONTRIBUTIONS

YBM, MG, TO, and NK conceived the study. YBM and TO performed experiments. MG and TO performed image processing. MG and YBM performed data analyses. MG conducted mathematical modeling and simulations. All authors discussed the results and contributed to the final manuscript. NK supervised the project. YBM, MG, TO, and NK wrote the manuscript.

COMPETING INTERESTS

The authors declare no competing interests.

ADDITIONAL INFORMATION

Supplementary information The online version contains supplementary material available at https://doi.org/10.1038/s41396-021-01051-4.

Correspondence and requests for materials should be addressed to N.K.

Reprints and permission information is available at http://www.nature.com/reprints

Publisher's note Springer Nature remains neutral with regard to jurisdictional claims in published maps and institutional affiliations.